

Step by Step: Using Step Selection Functions to Simulate Dispersal and Assess Landscape Connectivity

David D. Hofmann^{1,2,§} Gabriele Cozzi^{1,2} John W. McNutt² Arpat Ozgul¹
Dominik M. Behr^{1,2}

September 23, 2021

¹ Department of Evolutionary Biology and Environmental Studies, University of Zurich,
Winterthurerstrasse 190, 8057 Zurich, Switzerland.

² Botswana Predator Conservation, Private Bag 13, Maun, Botswana.

§ Corresponding author (david.hofmann2@uzh.ch)

Running Title: Release the Dogs! Simulating Wild Dog Dispersal to Assess Landscape
Connectivity

Keywords: dispersal, simulation, movement, integrated step selection function,
Kavango-Zambezi Transfrontier Conservation Area, landscape connectivity, *Lycaon pictus*

Abstract

Dispersal of individuals is crucial for long-term species persistence and depends on a sufficient degree of landscape connectivity. Thusfar, researchers have investigated connectivity primarily using least-cost analysis and circuit theory, although both methods make assumptions that are rarely met in reality. Least-cost analysis assumes that animals move towards a known endpoint and are knowledgeable about the least costly route to reach it. Circuit theory relies on the assumption of a complete random walk without any directional persistence along the dispersing route. Albeit these shortcomings can be overcome by spatio-temporally explicitly simulating dispersing trajectories across the landscape, a unified approach for such a simulation is lacking.

Here, we present a simple three-step workflow to simulate dispersal and assess connectivity starting from empirical GPS movement data. To exemplify its application, we employ the workflow to dispersal data collected on the endangered African wild dogs (*Lycaon pictus*) in the Kavango-Zambezi Transfrontier Conservation Area, the world's largest transboundary conservation area. In step one, we use integrated step selection functions to fit a mechanistic movement model describing habitat and movement preferences of dispersers. In step two, we apply the parameterized model to simulate individual dispersal trajectories. In step three, we compress the simulated trajectories into three complementary connectivity maps: a heatmap that highlights frequently traversed areas, a betweenness map that pinpoints dispersal corridors, and a map of interpatch connectivity, indicating the presence or absence of functional links between habitat patches.

Our results show that dispersing African wild dogs move with directional persistence in the vicinity to waterbodies and preferably through areas with little human influence. This is reflected in the simulation with resulted in several dispersal hotspots and corridors along waterbodies through areas with little or no anthropogenic pressure. Connectivity between national parks inside the KAZA-TFCA appears to be good, albeit the parks in Zambia and Zimbabwe are comparably less well connected to the rest of KAZA-TFCA, suggesting the necessity for additional protected areas that serve as "stepping stones" into these regions.

We show that simulations from step-selection functions offer a simple yet powerful alternative to traditional connectivity modeling techniques, although necessitating informed decisions about the number of simulated individuals and the duration of simulated dispersal events. Ultimately, our workflow permits a more mechanistic understanding of dispersal behaviour and landscape connectivity making it useful for a variety of applications in ecological, evolutionary, and conservation research.

Contents

1	Introduction	1
1.1	Importance of Connectivity & Connectivity Models	1
1.2	Issues with Traditional Connectivity Models	1
1.3	What about IBMMs?	2
1.4	Proposed Solution: Three-Step Workflow	2
1.5	Introduction of the Study Species	3
1.6	Case Study	3
2	Methods	3
2.1	Study Area	3
2.2	Data Collection and Preparation	4
2.2.1	GPS Data	4
2.2.2	Habitat Covariates	4
2.3	Step 1 - Movement Model	5
2.4	Step 2 - Dispersal Simulation	6
2.5	Step 3 - Connectivity Maps	8
2.5.1	Heatmap	8
2.5.2	Betweenness Map	8
2.5.3	Inter-Patch Connectivity Map	8
3	Results	9
3.1	Movement Model	9
3.2	Dispersal Simulation	10
3.3	Heatmap	10
3.4	Betweenness	10
3.5	Inter-Patch Connectivity	11
4	Discussion	11
4.1	Short Summary	11
4.2	Movement Model	12
4.3	Simulation	13
4.4	Maps	13
4.5	Related Literature	14
4.6	Advantages of ISSF Simulations	15
4.7	Disadvantages of ISSF Simulations	16
4.8	Conclusion	18
5	Authors' Contributions	18
6	Data Availability	18
7	Acknowledgements	19

1 Introduction

1.1 Importance of Connectivity & Connectivity Models

Dispersal of individuals is a vital process that allows species to maintain genetic diversity (Perrin and Mazalov, 1999, 2000; Frankham et al., 2002; Leigh et al., 2012; Baguette et al., 2013), rescue non-viable populations (Brown and Kodric-Brown, 1977), and colonize unoccupied habitats (Hanski, 1999; MacArthur and Wilson, 2001). However, the ability to disperse depends on a sufficient degree of landscape connectivity (Fahrig, 2003; Clobert et al., 2012), making the identification and protection of dispersal corridors that promote connectivity a task of fundamental importance (Nathan, 2008; Doerr et al., 2011; Rudnick et al., 2012). The identification of dispersal corridors not only necessitates a comprehensive understanding of the factors that limit dispersal, but also an appropriate model to estimate connectivity (Baguette et al., 2013; Vasudev et al., 2015; Hofmann et al., 2021). To date, the two most commonly used connectivity models are least-cost path analysis (LCPA; Adriaensen et al., 2003) and circuit theory (CT; McRae, 2006; McRae et al., 2008), both graph-based methods that quantify conductance of the landscape based on habitat permeability (Zeller et al., 2012). However, both approaches rest on assumptions that appear unsuitable for dispersers, which is why simulating dispersal from individual-based movement models provides a promising alternative approach to modeling connectivity (Diniz et al., 2019).

1.2 Issues with Traditional Connectivity Models

Traditional connectivity models make assumptions that are rarely met for dispersers. LCPA, for instance, assumes that individuals move towards a preconceived endpoint and choose a cost-minimizing route accordingly (Sawyer et al., 2011; Abrahms et al., 2017). While this assumption may be fulfilled by migrating animals, it is unlikely to hold for dispersers, as dispersers typically move across unfamiliar territory and are therefore less aware of associated movement costs and potential endpoints (Koen et al., 2014; Cozzi et al., 2020). CT, on the contrary, posits that animals move according to a random walk, entailing that autocorrelation between subsequent movements cannot be rendered (Diniz et al., 2019). For dispersers, however, autocorrelated movements are regularly observed (Cozzi et al., 2020; Hofmann et al., 2021), implying that subsequent relocations tend to fall onto a straight line. Moreover, graph-based methods are unable to reflect the temporal dimension of dispersal, meaning that statements about the approximate duration required to move between habitats is impossible (Martensen et al., 2017; Diniz et al., 2019).

³³ **1.3 What about IBMMs?**

³⁴ The shortcomings inherent to LCPA and CT can be overcome by simulating dispersal tra-
³⁵ jectories from individual-based movement models (IBMMs) and by converting simulated
³⁶ trajectories into meaningful measures of connectivity (Diniz et al., 2019)). IBMMs allow to
³⁷ explicitly simulate how individuals move across and interact with the encountered landscape
³⁸ (Kanagaraj et al., 2013; Clark et al., 2015; Allen et al., 2016; Hauenstein et al., 2019; Zeller
³⁹ et al., 2020) and to render potential interactions between movement behavior and habitat
⁴⁰ conditions. This shifts the focus from a structural to a more functional view on connectivity
⁴¹ (Tischendorf and Fahrig, 2000; Kanagaraj et al., 2013; Hauenstein et al., 2019). Furthermore,
⁴² simulations from IBMMs generate movement sequentially, making the temporal dimension
⁴³ of dispersal explicit and allowing to model autocorrelation between subsequent movements
⁴⁴ (Diniz et al., 2019). Finally, simulations from IBMMs do not enforce connections towards
⁴⁵ preconceived endpoints, thereby mitigating biases arising from misplaced endpoints. Despite
⁴⁶ these advantages, a unified framework to simulate dispersal and assess connectivity using
⁴⁷ IBMMs is lacking.

⁴⁸ **1.4 Proposed Solution: Three-Step Workflow**

⁴⁹ Here, we draw on recent advancements in the fields of movement ecology and network theory
⁵⁰ to propose a simple three-step workflow for simulating dispersal movements and assessing
⁵¹ landscape connectivity (Figure 1). In step one, we combine GPS movement data of dispers-
⁵² ing individuals with relevant habitat covariates to fit a mechanistic movement model using
⁵³ integrated step selection functions (ISSFs, Avgar et al., 2016). ISSFs permit simultaneous
⁵⁴ inference on the focal species' habitat kernel (i.e. habitat preferences), its movement kernel
⁵⁵ (i.e. movement preferences/capabilities), and potential interactions between the two (Avgar
⁵⁶ et al., 2016; Fieberg et al., 2021). In step two, we simulate individual dispersal trajectories
⁵⁷ using the movement model parametrized in step one. Finally, in step three, we convert simu-
⁵⁸ lated trajectories into three complementary connectivity maps, each highlighting a different
⁵⁹ aspect of connectivity. The proposed set of maps includes (i) a heatmap revealing areas
⁶⁰ that are frequently traversed by simulated dispersers (e.g. Hauenstein et al., 2019; Zeller
⁶¹ et al., 2020), (ii) a betweenness-map delineating dispersal corridors and bottlenecks (e.g.
⁶² Bastille-Rousseau et al., 2018), (iii) and a map of inter-patch connectivity, depicting the
⁶³ presence or absence and intensity of use of specific connections, and the average dispersal
⁶⁴ duration between corresponding habitat patches (e.g. Kanagaraj et al., 2013).

65 **1.5 Introduction of the Study Species**

66 The endangered African wild dog (*Lycaon pictus*) represents a highly mobile species whose
67 persistence hinges on a sufficient degree of landscape connectivity. Once common through-
68 out sub-Saharan Africa, this species has disappeared from much of its historic range, largely
69 due to human persecution, habitat fragmentation, and disease outbreaks (Woodroffe and
70 Sillero-Zubiri, 2012). Wild dogs typically emigrate in single-sex coalitions (McNutt, 1996;
71 Behr et al., 2020) capable of dispersing several hundred kilometers (Davies-Mostert et al.,
72 2012; Masenga et al., 2016; Cozzi et al., 2020). Although previous studies have investigated
73 connectivity using LCPA (Hofmann et al., 2021) or CT (Brennan et al., 2020), a more com-
74 prehensive and mechanistic understanding of connectivity is missing for this species (but
75 see Creel et al., 2020). With fewer than 6,000 free-ranging wild dogs remaining in frag-
76 mented populations (Woodroffe and Sillero-Zubiri, 2012), reliable information on landscape
77 connectivity is essential for the conservation of this endangered carnivore.

78 **1.6 Case Study**

79 In this study, we illustrate the proposed three-step workflow (Figure 1) to assess landscape
80 connectivity for African wild dogs within the Kavango-Zambezi Transfrontier Conservation
81 Area (KAZA-TFCA), the world’s largest transboundary conservation area. To this end,
82 we use GPS movement data of 16 dispersing wild dogs originating from a free-ranging
83 population in northern Botswana to parametrize a mechanistic movement model, which we
84 then employed to simulate 80,000 dispersal trajectories across the landscape of the KAZA-
85 TFCA. We anticipated that simulations based on our three-step workflow would overcome
86 several of the above highlighted conceptual shortcomings of traditional connectivity models
87 and provide a more comprehensive view of landscape connectivity.

88 **2 Methods**

89 **2.1 Study Area**

90 The study area centered at -17°13'9"S, 23°56'4"E (Figure 2a) is located in southern Africa
91 (Figure 2a) and spans more than 1.3 Mio. km², encompassing the entire KAZA-TFCA (Fig-
92 ure 2b). The KAZA-TFCA comprises parts of Angola, Botswana, Namibia, Zimbabwe, and
93 Zambia and hosts diverse landscapes; ranging from savannah to grassland and from dry to
94 moist woodland habitats. In its center lies the Okavango Delta, a dominant hydrogeographi-
95 cal feature and the world’s largest flood-pulsing inland delta. Although large portions of the

⁹⁶ KAZA-TFCA are part of designated national parks and other protected areas, considerable
⁹⁷ human influence from roads, agricultural sites, and settlements remains.

⁹⁸ 2.2 Data Collection and Preparation

⁹⁹ 2.2.1 GPS Data

¹⁰⁰ We collected GPS movement data on 16 dispersing wild dogs (7 females and 9 males) between
¹⁰¹ 2011 and 2019 from a free-ranging population in northern Botswana (details on the data
¹⁰² collection can be found in Cozzi et al. (2020) and Hofmann et al. (2021)). Because behavior
¹⁰³ during dispersal is more pertinent to landscape connectivity than behavior during residence
¹⁰⁴ (Elliot et al., 2014; Abrahms et al., 2017), we discarded data collected when individuals were
¹⁰⁵ resident. We determined the exact timing of emigration and settlement using direct field
¹⁰⁶ observations and through visual inspection of the net squared displacement (NSD) metric.
¹⁰⁷ NSD measures the squared Euclidean distance of a GPS relocation to a reference point
¹⁰⁸ (Börger and Fryxell, 2012), which we set to the center of each dispersers' natal home range.
¹⁰⁹ Thus, dispersal was deemed to have started once an individual left its natal home range and
¹¹⁰ ended once the NSD metric remained constant, indicating settlement. During dispersal, GPS
¹¹¹ collars recorded a fix every 4 hours and they regularly transmitted data over the Iridium
¹¹² satellite system. To ensure regular timespans between fixes, we removed any fix that was not
¹¹³ obtained on the aspired 4-hourly schedule (\pm 15 minutes). We then converted the remaining
¹¹⁴ fixes ($n = 4'169$) into steps, where each step represented the straight-line movement between
¹¹⁵ two consecutive GPS relocations (Turchin, 1998).

¹¹⁶ 2.2.2 Habitat Covariates

¹¹⁷ We represented the physical landscape in our study area by the habitat covariates *water-*
¹¹⁸ *cover*, *distance-to-water*, *woodland-cover*, *shrub/grassland-cover*, and *human-influence*. To
¹¹⁹ reflect the seasonality of water in the study area, we obtained weekly updated layers for
¹²⁰ water-cover and corresponding layers for distance-to-water from MODIS satellite imagery
¹²¹ using a remote sensing algorithm Wolski et al., 2017; Hofmann et al., 2021 that is im-
¹²² plemented in the `floodmapr` package which is available on GitHub (<https://github.com/DavidDHofmann/floodmapr>). For each step, we thus used the temporally associated water
¹²⁴ layers, reflecting prevailing conditions at the time when the step was realized. To ensure a
¹²⁵ consistent resolution across habitat covariates, we coarsened or interpolated all layers to a
¹²⁶ resolution of 250 m x 250 m. A more detailed description of how we prepared each habitat
¹²⁷ covariate is provided in Hofmann et al. (2021).

128 Besides habitat covariates, we computed movement metrics that we used as movement
 129 covariates in our ISSF analysis (Avgar et al., 2016; Fieberg et al., 2021). Movement metrics
 130 were calculated for each step and included the step length (`sl`), its natural logarithm (`log(sl)`),
 131 and the cosine of the relative turning angle (`cos(ta)`). Moreover, we created the binary
 132 variable `LowActivity` indicating whether a step was realized during periods of low wild dog
 133 activity (09:00 to 17:00 local time) or high wild dog activity (17:00 to 09:00 local time, Cozzi
 134 et al., 2012). We performed all data preparations, spatial computations, and statistical
 135 analysis in R, version 3.6.6 (R Core Team, 2020). Some helper functions were written in C++
 136 and imported into R using the `Rcpp` package (Eddelbuettel and François, 2011; Eddelbuettel,
 137 2013). We provide annotated R-codes to reproduce the three-step workflow using simulated
 138 data through GitHub (<https://github.com/DavidDHofmann/DispersalSimulation>). In
 139 addition, codes for the African wild dog case study are available through an online repository.

140 2.3 Step 1 - Movement Model

141 We used ISSFs to parametrize a mechanistic movement model for dispersing wild dogs
 142 (Avgar et al., 2016). More specifically, we paired each realized step with 24 random steps,
 143 so that a realized step plus its 24 random steps formed a stratum that received a unique
 144 identifier. As suggested by Avgar et al. (2016), we generated random steps by sampling
 145 random turning angles from a uniform distribution $(-\pi, +\pi)$ (which is equivalent to a von
 146 Mises distribution with concentration parameter $\kappa = 0$) and step lengths from a gamma
 147 distribution that was fitted to realized steps (scale $\theta = 6.308$ and shape $k = 0.37$). Along
 148 each step, we extracted and averaged values from the habitat covariate layers using the
 149 `velox` package (Hunziker, 2021) and calculated the movement metrics `sl`, `log(sl)`, and `cos(ta)`
 150 for each realized and random step. To facilitate model convergence, we standardized all
 151 continuous covariates to a mean of zero and a standard deviation of one. Since correlation
 152 among covariates was low ($|r| < 0.6$; Latham et al., 2011), we retained all of them for
 153 modeling.

154 To contrast realized steps (scored 1) and random steps (scored 0), we assumed that
 155 animals assigned a selection score $w(x)$ of the exponential form to each step (Fortin et al.,
 156 2005). $w(x)$ depended on the step's associated covariates (x_1, x_2, \dots, x_n) and on the animal's
 157 preferences (i.e. relative selection strengths; Avgar et al., 2017) towards these covariates
 158 $(\beta_1, \beta_2, \dots, \beta_n)$:

$$w(x) = \exp(\beta_1 x_1 + \beta_2 x_2 + \dots + \beta_n x_n) \quad (\text{Equation 1})$$

159 The probability of a step being realized was then contingent on the step's selection score,
160 as well as on the selection scores of all other step in the same stratum:

$$P(Y_i = 1|Y_1 + Y_2 + \dots + Y_i = 1) = \frac{w(x_i)}{w(x_1) + w(x_2) + \dots + w(x_i)} \quad (\text{Equation 2})$$

161 To estimate preferences (i.e. the β -coefficients), we used mixed effects conditional logistic
162 regression analysis (Muff et al., 2020) that we implemented using the r-package `glmmTMB`
163 (Brooks et al., 2017). To capitalize on the poisson trick introduced by Muff et al. (2020), we
164 defined random intercepts for each stratum and fixed the intercept variance to an arbitrary
165 high value of 10^{**6} . We also used disperser identity to model random slopes for all covariates.

166 The covariate structure of the movement model was based on a habitat selection model
167 that we previously developed (hereafter referred to as base model, Hofmann et al., 2021).

168 In the base model, no interactions among habitat covariates and movement covariates were
169 considered. Hence, we expanded the base model and allowed for interactions between all
170 movement covariates and habitat covariates, thus reflecting that movement behavior may
171 depend on habitat conditions (details in Appendix AX). To assess the most parsimonious
172 movement model among model candidates, we ran stepwise forward model selection based
173 on Akaike's Information Criterion (AIC, Burnham and Anderson, 2002). Finally, we val-
174 idated the predictive power of the most parsimonious model using k-fold cross-validation
175 for case-control studies as described in Fortin et al. (2009). In brief, this validation proofs a
176 significant prediction in case the Spearman rank correlation of predicted step ranks and as-
177 sociated frequencies under the movement model is significantly stronger than under random
178 preferences (details in Appendix AX).

179 2.4 Step 2 - Dispersal Simulation

180 We used the most parsimonious movement model to simulate individual dispersal trajec-
181 tories within the study area. The simulation of a dispersal trajectory resembled an “inverted”
182 ISSF and was set up as follows. (1) We defined a random source point and assumed a
183 random initial orientation of the animal. (2) Starting from the source point, we generated
184 25 random steps by sampling turning angles from a uniform distribution $(-\pi, +\pi)$ and step
185 lengths from our fitted gamma distribution. Like in the empirical data, each random step
186 represented the straight line movement possible within 4 hours. To prevent unreasonably
187 large steps, we restricted sampled step lengths to a maximum of 35 km (i.e. the farthest
188 dispersal distance traveled within 4 hours in our data). (3) Along each random step, we

189 extracted and averaged values from the respective habitat covariate layers and calculated
190 movement covariates. To ensure compatible scales with the fitted movement model, we
191 standardized extracted values using the mean and standard deviation from the empirical
192 data. (4) We applied the parametrized movement model to predict the selection score $w(x)$
193 for each step and we translated predicted scores into probabilities using Equation 2. (5) We
194 used predicted probabilities to sample one of the random steps and determined the animal's
195 new position. We repeated steps (2) to (5) until 2,000 steps (i.e. 400 consecutive dispersal
196 days) were realized.

197 To mitigate edge effects and to deal with random steps leaving the study area, we followed
198 Koen et al. (2010) and artificially expanded all covariate layers by a 100 km wide buffer
199 zone. Within the buffer zone, we randomized covariate values by resampling values from
200 the original covariate layers. Through this buffer zone, simulated dispersers were able to
201 leave and re-enter the main study area. In cases where proposed random steps transgressed
202 the outer border of this buffer zone, we resampled transgressing steps until they fully lied
203 within the buffer zone, forcing individuals to remain within the expanded study area.

204 For the simulation, we distributed 80,000 unique source points within the study area. Of
205 these, 50,000 were random locations inside protected areas that were larger than the average
206 home range size of wild dogs (i.e. $> 700 \text{ km}^2$; Pomilia et al., 2015), while the remaining
207 30,000 source points were placed randomly inside the buffer zone, mimicing potential immi-
208 gration into the study area (Figure S1). Due to the random distribution of source points,
209 the number of source points per km^2 in selected areas was approximately equal.

210 To ensure reliable connectivity estimates, we determined the number of simulated dis-
211 persal trajectories required for connectivity to reach a "steady state" across the entire study
212 area. For this purpose, we distributed 1,000 rectangular "checkpoints", each with an extent
213 of 5 km x 5 km at random coordinates within the study area (excluding the buffer). We
214 then determined the relative frequency at which each checkpoint was traversed by simulated
215 dispersers (hereafter referred to as relative traversal frequency) as we gradually increased the
216 number of simulated trajectories from 1 to 50,000. To assess variability in the relative traver-
217 sal frequency, we repeatedly subsampled 100 times from all 50'000 dispersal trajectories and
218 computed the mean traversal frequency across replicates, as well as its 95% confidence-
219 interval for each checkpoint. We considered connectivity to have reached a steady state
220 once the width of the prediction-interval dropped below a value of 0.01 for all checkpoints.

Since we did not explain the 8-hourly gaps, this might be confusing

221 **2.5 Step 3 - Connectivity Maps**

222 **2.5.1 Heatmap**

223 To identify dispersal hotspots within the study area, we created a heatmap indicating the
224 absolute frequency at which each raster-cell was traversed by simulated dispersers (e.g. Pe'er
225 and Kramer-Schadt, 2008; Hauenstein et al., 2019; Zeller et al., 2020). That is, we rasterized
226 all simulated trajectories onto a raster with 250 m x 250 m resolution and tallied them into
227 a single map. If the same trajectory crossed a raster-cell twice, we only counted it once,
228 thereby mitigating biases from individuals that were trapped and moved in circles. To
229 achieve high performance rasterization, we used the R-package **terra** (Hijmans, 2021).

230 **2.5.2 Betweenness Map**

231 To pinpoint discrete movement corridors and bottlenecks, we converted simulated trajectories
232 into a network and calculated betweenness scores for all raster-cells in the study area
233 (Bastille-Rousseau et al., 2018). Betweenness measures how often a specific network-node
234 (i.e. raster-cell) lies on a shortest path between any other pair of nodes and is therefore
235 pertinent to connectivity (Bastille-Rousseau et al., 2018). To transform simulated trajectories
236 into a network, we followed (Bastille-Rousseau et al., 2018) and overlaid the study area
237 (including the buffer) with a 5 km x 5 km raster, where the center of each raster-cell served
238 as node in the final network. To identify edges (i.e. connections) between the nodes, we
239 used the simulated trajectories and determined all transitions occurring from one node to
240 another, as well as the frequency at which those transitions occurred. This resulted in an
241 edge-list that we translated into a weighted network using the r-package **igraph** (Csardi and
242 Nepusz, 2006). The weight of each edge was determined by the frequency of transitions, yet
243 because **igraph** handles edge weights (ω) as costs, we had to invert the traversal-frequency
244 thorough each raster-cell by applying $\omega = \frac{\text{mean}(\text{TraversalFrequency})}{\text{TraversalFrequency}_i}$. Consequently, edges that
245 were traversed frequently were assigned small weights and vice versa. Finally, we used the
246 weighted network to calculate betweenness scores at all network nodes.

247 **2.5.3 Inter-Patch Connectivity Map**

248 To examine the presence and intensity of functional links (i.e. connections) between specific
249 patches inside the KAZA-TFCA, we calculated inter-patch connectivity between national
250 parks. The decision to only consider national parks as our “patches” was purely out of
251 simplicity and does not imply that connections between other protected areas are impos-
252 sible. To quantify inter-patch connectivity, we computed the relative frequency at which

253 dispersers originating from one national park successfully moved into another national park.
254 We considered movements successful if the individuals' dispersal trajectory intersected with
255 the target national park at least once. We also recorded the number of steps required to
256 reach the first intersection with the respective national park, allowing us to compute the
257 average dispersal durations from one park to another. In summary, we determined *if* and
258 *how often* dispersers moved between certain national parks, as well as *how long* individuals
259 had to move to make these connections.

260 3 Results

261 3.1 Movement Model

262 The most parsimonious movement model consisted of movement covariates, habitat covari-
263 ates and several of their interactions, suggesting that movement behavior during dispersal
264 depends on habitat conditions (Figure 3, Table S1 and Table S2). Although multiple models
265 received an AIC weight $\gtrsim 0$ (Table S1), we only considered results from the most parsimo-
266 nious model for simplicity. This decision only marginally influenced subsequent steps as all
267 models with positive AIC weights contained similar covariates (Table S1). Aids for inter-
268 preting main effects and interactions are provided in Figure S2. Under average conditions,
269 dispersing wild dogs avoided moving through water, woodlands, and areas dominated by
270 humans, but preferred shrublands or grasslands (Figure 3). Dispersers realized shorter steps
271 (indicating slower movements) in areas covered by water or woodland, while realizing larger
272 steps in areas dominated by shrubs or grass. Moreover, dispersing wild dogs moved faster
273 during twilight and at night (i.e. between 17:00 and 09:00 o'clock) than during the rest
274 of the day. Although dispersers showed a preference for directional movements, especially
275 when moving quickly, they did less so in proximity to humans or water, resulting in more
276 tortuous movements in such areas.

277 The k-fold cross-validation of the movement model showed that the final model substan-
278 tially outperforms a random guess , suggesting reliable predictions (confidence intervals of
279 $\bar{r}_{s,realized}$ and $\bar{r}_{s,random}$ do not overlap). Moreover, the model correctly assigns high se-
280 lection scores to realized steps (Figure 3b), indicating a good fit between predictions and
281 observations. Compared to the base model ($\bar{r}_{s,realized} = -0.55; 95\% - CI = [-0.57, -0.52]$;
282 Hofmann et al., 2021), the inclusion of several interactions between movement and habi-
283 tate covariates significantly improved model performance ($\bar{r}_{s,realized} = -0.65; 95\% - CI =$
284 $[-0.67, -0.64]$).

285 **3.2 Dispersal Simulation**

286 Our dispersal simulations based on the most parsimonious movement model proved useful
287 for assessing landscape connectivity. Of the 50,000 simulated dispersers initiated within
288 the main study area, only 4.5% were eventually repelled by a map boundary, suggesting
289 minimal biases due to boundary effects. Moreover, our examination of relative traversal
290 frequencies across all checkpoints suggested that connectivity reached a steady state after
291 10,500 simulated dispersal trajectories (Figure S3). Although variability in relative traversal
292 frequencies kept decreasing as we increased the number of simulated dispersers, the marginal
293 benefit of additional trajectories diminished quickly (Figure S3).

294 **3.3 Heatmap**

295 The heatmap (Figure 4), which resulted from the summation of all simulated dispersal
296 trajectories, showed that several extensive regions within the KAZA-TFCA were frequently
297 traversed by dispersing wild dogs (mean traversal frequency = 166, IQR = 274, Figure S6a),
298 while areas beyond the KAZA-TFCA boundary were rarely visited (mean traversal frequency
299 = 61, IQR = 133, Figure S6a). Most notably, the region in northern Botswana south of the
300 Linyanti swamp appeared as highly frequented dispersal hotspot (mean traversal frequency =
301 987, IQR = 558). Nevertheless, the presence of extensive water bodies, such as the Okavango
302 Delta, the Makgadikgadi Pan, and the Linyanti swamp, restricted dispersal movements
303 and limited realized connectivity within the KAZA-TFCA. Similarly, high human densities,
304 roads, and agricultural activities in Zambia's and Zimbabwe's part of the KAZA-TFCA
305 limited dispersal movements. Outside the KAZA-TFCA, the most heavily used regions
306 included the areas inside the Central Kalahari National Park in Botswana, the area south-
307 west of the Khaudum National Park in Namibia, and the area surrounding the Liuwa Plains
308 National Park in Zambia. Although the heatmap facilitated the identification of areas
309 frequently traversed by simulated dispersers, it seemed impractical to pinpoint dispersal
310 corridors.

311 **3.4 Betweenness**

312 The betweenness map (Figure 5) revealed distinct dispersal corridors that run within the
313 KAZA-TFCA . Again, the region in northern Botswana emerged as wild dog dispersal hub
314 that connected more remote regions in the study area. Towards east, the extension of
315 this corridor ran through Chobe National Park into Hwange National Park. From there, a
316 further extension connected to Matusadona National Park in Zimbabwe. Northwest of the

317 Linyanty ecosystem, a major corridor expanded into Angola, where it splitted and finally
318 traversed over a long stretch of unprotected area into Zambia's Kafue National Park. Several
319 additional corridors with lower betweenness scores emerged, yet most of them ran within
320 the KAZA-TFCA boundaries (median betweenness inside KAZA-TFCA = 6947k, IQR =
321 54311k, Figure S6b). In general, there were few corridors that directly linked the peripheral
322 regions of the KAZA-TFCA and passed through unprotected areas outside the KAZA-TFCA
323 (mean betweenness outside KAZA = 2685k, IQR = 9891k, Figure S6b). Compared to the
324 heatmap, the betweenness map facilitated the identification of dispersal corridors between
325 habitat patches.

326 **3.5 Inter-Patch Connectivity**

327 Results from the analysis of inter-patch connectivity are given in Figure 6, which shows all re-
328 alized links by simulated dispersers between national parks. The map furthermore indicates
329 the relative frequency at which dispersers originating from one national park successfully
330 reached another national park, as well as the average duration dispersers had to move to
331 realize those links. It is again worth pointing out that the figure is only intended as an il-
332 lustration, as for clarity we only considered inter-patch connectivity between national parks
333 (NPs), albeit plenty of links between other protected areas exist. Overall, inter-patch con-
334 nectivity between NPs in Angola, Namibia, and Botswana appears to be high, with relatively
335 short dispersal durations between national parks. In contrast, we observe that connections
336 from the central region into the Kafue NP in Zambia require rather long dispersal events and
337 are rather infrequent. Similarly, relatively few connections lead into Zimbabwe's Chizarira
338 and Matusadona NP. In some cases, we also find imbalances between ingoing and outgoing
339 links, hinting at potential source-sink dynamics that occur due to asymmetries in disperser's
340 willingness to cross an area, depending on the direction in which the area is traversed. For
341 instance, while a fair share of dispersers originating from the Chizaria NP in Zimbabwe
342 manages to move into the Hwange NP, there are comparably few dispersers that succeed in
343 the opposite direction.

344 **4 Discussion**

345 **4.1 Short Summary**

346 We used ISSFs to analyse data of dispersing wild dogs and to parametrize a fully mech-
347 anistic movement model describing how dispersers move through the available landscape.

348 We employed the parametrized model as an individual-based movement model to simulate
349 80'000 dispersing wild dogs moving 2'000 steps across the extent of the KAZA-TFCA, the
350 world's largest transboundary conservation area. Based on simulated dispersal trajectories,
351 we derived three complementary maps, each geared towards a better understanding
352 of dispersal and landscape connectivity. The set of maps included a heatmap, revealing
353 frequently traversed areas, a betweenness-map, delineating critical dispersal corridors, and
354 a map of inter-patch connectivity, indicating the presence or absence of functional links be-
355 tween national parks as well as the average dispersal duration required to realize those links.
356 We thereby showcase that ISSFs offer a simple, yet powerful framework to parametrize
357 movement models and simulate dispersal to assess landscape connectivity. Importantly,
358 individual-based simulations from ISSFs overcome several conceptual shortcomings inherent
359 to more traditional connectivity modeling techniques, such as LCPA and CT.

360 4.2 Movement Model

361 Because our movement model of dispersing wild dogs comprised two interacting kernels, it
362 effectively rendered habitat and movement preferences of dispersers, as well as how pref-
363 erences depended on habitat conditions. Results from the habitat kernel were largely in
364 concert with previous studies that investigated habitat selection by dispersing wild dogs
365 (Davies-Mostert et al., 2012; Masenga et al., 2016; Woodroffe et al., 2019; O'Neill et al.,
366 2020; Hofmann et al., 2021). However, by also incorporating a movement kernel, we were
367 able to model several additional complexities inherent to dispersal. For instance, we could
368 accommodate that dispersers move with directional persistence (Cozzi et al., 2018; Hofmann
369 et al., 2021) and exhibit step lengths that are correlated with turning angles (Morales et al.,
370 2004; Börger and Fryxell, 2012) by including the appropriate interactions in the movement
371 model. While correlations between step lengths and turning angles could also be rendered
372 by sampling them from copula probability distributions (Hodel and Fieberg, 2021a,b), the
373 ISSF framework allowed us to directly incorporate them in the movement model. In addi-
374 tion, by forming interactions between habitat covariates and movement covariates, we could
375 render potential dependencies between movement and habitat preferences. For example,
376 our final model contained an interaction between water-cover and step length, showing that
377 dispersers realize shorter steps in areas covered by water. Likewise, we found that dispersers
378 move more tortuously across water bodies than over dryland, which is clearly to be expected,
379 given that wild dogs have to wade or swim when traversing waterbodies. The ability of ac-
380 companying such effects in a single model is one of the great strengths of ISSFs (Avgar et al.,

381 2016; Fieberg et al., 2021), which is why we believe the method offers a suitable framework
382 for simulating movement and assessing connectivity.

383 4.3 Simulation

384 Our simulation of 80'000 dispersers moving 2'000 steps across the landscapes of the KAZA-
385 TFCA required five days of computation on a modern desktop machine.

386 On a machine with an octa-core AMD Ryzen 7 2700X processor (8 x 3.6 GHz, 16 logical
387 cores) and 64 GB of RAM, a batch of 1'000 simulated dispersers moving over 2'000 steps
388 required 90 minutes to compute ($\mu = 88.90$, $\sigma = 1.87$). Consequently, the simulation of all
389 80'000 dispersers (160 Mio. steps) terminated after 120 hours (i.e. five days). Comparable
390 simulations will be substantially faster for smaller study areas and lower resolution covari-
391 ates, as the covariate extraction from large and high-resolution rasters was computationally
392 the most demanding task. Out of the 50'000 dispersers initiated inside the main source
393 area, only 4.5% were eventually repelled by a map boundary, suggesting that biases due to
394 boundary effects should be minimal.

395 The long simulation time was primarily caused by the massive extent considered (ca. 1.8
396 Mio. km² when including the buffer) and the large number of dispersers simulated. Most
397 connectivity studies are limited to much smaller extents (e.g. Kanagaraj et al., 2013; Clark
398 et al., 2015; McClure et al., 2016; Abrahms et al., 2017; Zeller et al., 2020) and will therefore
399 achieve faster simulation times. We also believe that fewer simulated dispersers will often
400 suffice, as the relative traversal frequency by simulated individuals through randomly placed
401 checkpoints in the study area converged already after 10'500 simulated individuals. However,
402 the required number of simulated individuals to achieve reliable estimates of connectivity
403 will vary depending on the structure of the landscape and the dispersal ability of the focal
404 species.

405 4.4 Maps

406 The heatmap generated from simulated dispersal trajectories highlighted that numerous
407 individuals traversed the Moremi NP and the Chobe NP in northern Botswana. We pre-
408 viously uncovered the same area as potential dispersal hotspot using least-cost methods
409 (Hofmann et al., 2021), yet it has been questioned whether this was a consequence of the
410 region being located in the center of the study area and connections being enforced between
411 predefined start and endpoints. With the current simulations, connections were no longer
412 enforced and simulated individuals were able to leave the main study area. Nonetheless, a

413 majority of simulated individuals traversed the area in northern Botswana. This suggests
414 that the dispersal hotspot is not merely an artifact of the applied method but truly results
415 from landscape characteristics. The same region is also pronounced on the betweenness
416 map, implying that it facilitates the relocation of individuals into more remote regions of
417 the KAZA-TFCA. While this is an example of an area where both the heatmap and the
418 betweenness map attest great importance, there are other instances where this is not true.
419 For example, while the area between the Lengue-Luiana NP in Angola and the Kafue NP in
420 Zambia receives a high betweenness-score, the heatmap shows that the area is only rarely
421 traversed by dispersers. Hence, despite the region's importance for linking Angola's NPs
422 to Zambia's NP, only few simulated dispersers actually used the corridor. Conversely, we
423 find that the Central Kalahari NP receives a low betweenness score, despite being highly
424 frequented by simulated dispersers. Besides highlighting frequently traversed areas and dis-
425 persal corridors, we also also consulted inter-patch connectivity between NPs, depicting the
426 presence or absence of functional links between national parks. Because dispersal move-
427 ments were rendered sequentially, we could also derive the average dispersal duration that
428 was required to realize those links. This enabled us to show that movements from Angola
429 into Zambia's Kafue NP are rare and require a large number of steps , whereas dispersal
430 between the Moremi NP and Chobe NP occurs frequently and requires relatively few steps.
431 All in all, the rich inference that can be drawn from the ensemble of proposed connectivity
432 maps.

433 4.5 Related Literature

434 Our approach of simulating movement to assess connectivity is related to a series of previ-
435 ously published papers. Clark et al. (2015), for instance, collected GPS data on American
436 black bears (*Ursus americanus*) and used SSFs to fit a habitat selection model. They then
437 used the fitted model to simulate movement and identify likely movement corridors between
438 four distinct habitat patches. For the same species, Zeller et al. (2020) used SSFs and
439 forecasted seasonal habitat connectivity under changing land-use. Because both of these
440 studies relied on *regular* SSFs, rather than *integrated* SSFs, they could not account for in-
441 terdependencies among habitat and movement preferences (Avgar et al., 2016). In addition,
442 both studies employed data collected on resident individuals instead of dispersers, although
443 evidence suggests that residents are more reluctant to cross areas that are readily traversed
444 by dispersers (Elliot et al., 2014; Gastón et al., 2016; Abrahms et al., 2017; Keeley et al.,
445 2017). The application of data collected on resident animals may therefore result in an

446 underestimate of connectivity (Elliot et al., 2014). Two further studies that used SSFs to
447 simulate animal movement have been conducted by Potts et al. (2013) and Signer et al.
448 (2017), yet the primary purpose here was to estimate steady-state utilization distributions
449 of resident animals and not on the analysis of dispersal and connectivity.

450 **4.6 Advantages of ISSF Simulations**

451 A simulation-based approach as proposed in this article offers several advantages over LCRA
452 and CT. In contrast to LCRA, for instance, an individual-based simulation does not require
453 to assume known endpoints. Instead, each endpoint emerges naturally from a simulated dis-
454 persal trajectory. The ability of not needing to provide endpoints is particularly valuable for
455 dispersal studies, because dispersers often venture into unfamiliar territory and are therefore
456 unlikely to know the destination of their journey (Elliot et al., 2014; Abrahms et al., 2017;
457 Cozzi et al., 2020). Moreover, LCRA always enforces a connection towards the pre-defined
458 endpoints, even if associated movement costs are unreasonably high. With simulations from
459 ISSFs this is no longer the case. A connectivity model that does not require pre-defined
460 endpoints also ensures that movement corridors are not enforced between certain start- and
461 endpoints, which permits to detect potential routes that do not lead into suitable habitats
462 but into ecological traps (Dwernychuk and Boag, 1972; Van der Meer et al., 2014) or areas
463 with a high susceptibility for human wildlife conflicts (Cushman et al., 2018).

464 In contrast to LCRA and CT, simulations from ISSFs furthermore yield the advantage
465 of an explicit representation of time, which enables to answer questions such as: “*How long*
466 *will it take a disperser to move from A to B?*” or “*Is it possible for a disperser to move*
467 *from A to B within X days?*”. An explicit representation of time also yields opportunities
468 for studying how seasonality affects connectivity and to investigate whether some dispersal
469 corridors are only available temporarily (*dynamic connectivity*; Zeller et al., 2020). With
470 LCRA or CT, incorporating seasonality is currently impractical, as both methods require a
471 static permeability surface as inputs. Hence, the only possibility to study seasonality effects
472 is to repeat the same analysis using different permeability surfaces, each rendering the
473 environment at a different point in time (e.g. Benz et al., 2016; Osipova et al., 2019). With
474 simulations from ISSFs, on the other hand, the environment can be rendered dynamically “as
475 the dispersers move”, such that simulated individuals can respond to seasonal factors directly
476 within the simulation. Hence, rather than employing a set of static habitat layers, each layer
477 would be updated as the dispersers move, thus correctly rendering seasonal changes in the
478 environment.

479 While an explicit representation of time provides several benefits, it requires that step
480 lengths and turning angles are modeled properly (Kanagaraj et al., 2013), so that dispersal
481 durations between areas can be estimated reliably. Correctly rendering step lengths and
482 turning angles under varying environmental conditions is one of the key strengths of ISSFs
483 (Avgar et al., 2016; Prokopenko et al., 2017; Fieberg et al., 2021), which is why we believe
484 that the framework is exceptionally well suited for simulating dispersal and assessing land-
485 scape connectivity. In addition, the framework enables to model autocorrelation between
486 step lengths and turning angles, thereby incorporating directional persistence. Here, we
487 only considered first order autocorrelation, i.e. correlation between two consecutive steps.
488 Although higher order autocorrelation is conceivable and might be desirable to model, this
489 requires vast amounts of GPS data that is not intercepted by missing fixes and is therefore
490 often impractical to model in reality.

491 4.7 Disadvantages of ISSF Simulations

492 Despite the benefits that simulations from ISSFs offer, we also want to confer some of the
493 non-trivial modeling decisions involved.

494 In particular, it is worth pointing out five modeling decisions: (1) number of simulated
495 individuals, (2) location of source points, (3) dispersal duration, (4) boundary behavior, and
496 (5) how to handle uncertainty and individual variability.

497 (1) When simulating dispersal, the modeler needs to decide on the number of simulated
498 individuals. A higher number is always desirable, as each additional disperser provides novel
499 information about landscape connectivity. However, this comes at the cost of computational
500 efficiency, implying that a trade-off needs to be managed. As noted by Signer et al. (2017),
501 the trade-off can be handled by simulating additional individuals only until estimated met-
502 rics converge. Here, we employed the relative traversal frequency across checkpoints as
503 target metric and found that convergence across all checkpoints was already achieved after
504 10'500 simulated individuals, yet we recognize that this strongly depends on the focal species
505 dispersal ability and landscape characteristics.

506 (2) Aside from specifying the absolute number of simulated individuals, one also needs to
507 define a source point within a suitable source area for each individual. Here, we placed source
508 points within protected areas large enough to sustain viable wild dog populations. Given
509 that wild dogs primarily survive in formally protected areas (Woodroffe and Ginsberg, 1999;
510 Davies-Mostert et al., 2012; Woodroffe and Sillero-Zubiri, 2012; Van der Meer et al., 2014)
511 we considered this decision to be appropriate. Due to a lack of precise knowledge about

512 wild dog abundances in the different protected areas, we distributed source points randomly
513 within them. If, however, corresponding data is available, source points can be distributed
514 accordingly, reflecting the fact that source areas do not necessarily produce an identical
515 number of dispersers. Alternatively, source points can be distributed homogeneously, but
516 be weighted afterwards according to estimated densities in the respective source area. In
517 cases where knowledge about suitable source areas is lacking, these could also be delineated
518 using habitat suitability models (e.g. Squires et al., 2013). After all, the challenge of selecting
519 meaningful source areas and source points is not unique to individual-based simulations and
520 also applies to LCPA or CT.

521 (3) When employing ISSFs to simulate dispersers, it is also required to decide on mean-
522 ingful dispersal durations (i.e. number of simulated steps). When sufficient dispersal data
523 of the focal species is available, dispersal durations can be sampled from observed dispersal
524 events. Due to the low number of observed dispersal events and due to the great variability
525 in wild dogs' dispersal distances (Davies-Mostert et al., 2012; Masenga et al., 2016; Cozzi
526 et al., 2020) we opted against this approach. Instead, we simulated individuals for 2'000
527 steps, which is at the upper end of observed dispersal durations. Once the trajectories have
528 been simulated, it is straightforward to subsample them and investigate the sensitivity of
529 derived results with regards to different dispersal durations.

530 (4) Unless simulated individuals are strongly drawn towards a point of attraction (e.g.
531 Signer et al. (2017)), dispersers eventually approach a map boundary, so that one or several
532 of the proposed random steps leave the study area. In theoretical applications, this issue can
533 be circumvented by simulating movement on a torus (?). For real data, however, alternative
534 solutions are needed. One approach would be to terminate the simulation, assuming that
535 the simulated animal left the study area forever. This can be problematic for individuals
536 that are initiated in areas that are located close to map boundaries, especially since already
537 a single random step leaving the study area breaks the simulation. Here, instead of breaking
538 the simulation loop, we simply resampled transgressing random steps until they fully lied
539 within the study area. This enforced simulated dispersers to be repelled by map boundaries
540 and to remain within the main study area. Additionally, we artificially increased the study
541 area using a buffer zone with randomized covariate values. This enabled virtual dispersers
542 to leave and re-enter the main study area. The same method has been shown to effectively
543 mitigate edge effects for graph-based connectivity models (Koen et al., 2010).

544 (5) We simulated dispersal using point estimates from our most parsimonious movement
545 model. Depending on the amount of data and individual variability, these estimates can be

546 subject to substantial uncertainty. For dispersal studies in particular, the low amount of
547 data typically results in model coefficients with large confidence intervals (Wiegand et al.,
548 2003; Kramer-Schadt et al., 2007). In these cases, point estimates may lead to biased
549 connectivity estimates, which is why we urge future studies to investigate the sensitivity
550 of ISSF simulations with respect to employed model parameters and to simulate dispersal
551 based on parameters that encapsulate model uncertainty.

552 **4.8 Conclusion**

553 To this end, we proposed and applied a simple three-step workflow that uses ISSFs to
554 parametrize an individual-based movement model from which dispersal can be simulated
555 with the purpose of informing about landscape connectivity. By explicitly simulating dis-
556 persal trajectories, simulations enable a more mechanistic understanding of connectivity,
557 and overcome several of the unrealistic assumptions inherent to graph-based connectivity
558 models, such as least-cost analysis or circuit theory. We exemplified the application of the
559 proposed workflow using data of dispersing wild dogs to assess landscape connectivity for
560 the species within the KAZA-TFCA ecosystem. With this, we hope to have sparked interest
561 in the powerful framework of step selection functions for investigating dispersal behavior
562 and landscape connectivity. Nevertheless, we propose to view simulations from ISSF-models
563 as complementary and not as substitutes to traditional connectivity modeling techniques.

564 **5 Authors' Contributions**

565 D.D.H., D.M.B., A.O. and G.C. conceived the study and designed methodology; D.M.B.,
566 G.C., and J.W.M. collected the data; D.D.H. and D.M.B. analysed the data; G.C. and A.O.
567 assisted with modeling; D.D.H., D.M.B., and G.C. wrote the first draft of the manuscript and
568 all authors contributed to the drafts at several stages and gave final approval for publication.

569 **6 Data Availability**

570 GPS movement data of dispersing wild dogs will be made available on dryad at the time of
571 publication. Access to R-scripts that exemplify the application of the proposed framework
572 to simulated data are provided through Github.

⁵⁷³ **7 Acknowledgements**

⁵⁷⁴ We thank the Ministry of Environment and Tourism of Botswana for granting permission to
⁵⁷⁵ conduct this research. We thank C. Botes, I. Clavadetscher, and G. Camenisch for assisting
⁵⁷⁶ with wild dog immobilizations. We also thank B. Abrahms for sharing her data of three
⁵⁷⁷ dispersing wild dogs. Furthermore, we are indebted to Johannes Signer for assisting with the
⁵⁷⁸ simulation algorithm. This study was funded by Basler Stiftung für Biologische Forschung,
⁵⁷⁹ Claraz Foundation, Idea Wild, Jacot Foundation, National Geographic Society, Parrotia
⁵⁸⁰ Stiftung, Stiftung Temperatio, Wilderness Wildlife Trust Foundation, Forschungskredit der
⁵⁸¹ Universität Zürich, and a Swiss National Science Foundation Grant (31003A_182286) to A.
⁵⁸² Ozgul.

583 References

- 584 Abrahms, B., Sawyer, S. C., Jordan, N. R., McNutt, J. W., Wilson, A. M., and Brashares,
585 J. S. (2017). Does Wildlife Resource Selection Accurately Inform Corridor Conservation?
586 *Journal of Applied Ecology*, 54(2):412–422.
- 587 Adriaensen, F., Chardon, J., De Blust, G., Swinnen, E., Villalba, S., Gulinck, H., and
588 Matthysen, E. (2003). The Application of Least-Cost Modelling as a Functional Landscape
589 Model. *Landscape and Urban Planning*, 64(4):233–247.
- 590 Allen, C. H., Parrott, L., and Kyle, C. (2016). An Individual-Based Modelling Approach to
591 Estimate Landscape Connectivity for Bighorn Sheep (*Ovis canadensis*). *PeerJ*, 4:e2001.
- 592 Avgar, T., Lele, S. R., Keim, J. L., and Boyce, M. S. (2017). Relative Selection Strength:
593 Quantifying Effect Size in Habitat- and Step-Selection Inference. *Ecology and Evolution*,
594 7(14):5322–5330.
- 595 Avgar, T., Potts, J. R., Lewis, M. A., and Boyce, M. S. (2016). Integrated Step Selection
596 Analysis: Bridging the Gap Between Resource Selection and Animal Movement. *Methods
597 in Ecology and Evolution*, 7(5):619–630.
- 598 Baguette, M., Blanchet, S., Legrand, D., Stevens, V. M., and Turlure, C. (2013). Indi-
599 vidual Dispersal, Landscape Connectivity and Ecological Networks. *Biological Reviews*,
600 88(2):310–326.
- 601 Bastille-Rousseau, G., Douglas-Hamilton, I., Blake, S., Northrup, J. M., and Wittemyer,
602 G. (2018). Applying Network Theory to Animal Movements to Identify Properties of
603 Landscape Space Use. *Ecological Applications*, 28(3):854–864.
- 604 Behr, D. M., McNutt, J. W., Ozgul, A., and Cozzi, G. (2020). When to Stay and When
605 to Leave? Proximate Causes of Dispersal in an Endangered Social Carnivore. *Journal of
606 Animal Ecology*, 89(10):2356–2366.
- 607 Benz, R. A., Boyce, M. S., Thurfjell, H., Paton, D. G., Musiani, M., Dormann, C. F., and
608 Ciuti, S. (2016). Dispersal Ecology Informs Design of Large-Scale Wildlife Corridors.
609 *PLOS ONE*, 11(9):e0162989.
- 610 Brennan, A., Beytell, P., Aschenborn, O., Du Preez, P., Funston, P., Hanssen, L., Kilian,
611 J., Stuart-Hill, G., Taylor, R., and Naidoo, R. (2020). Characterizing Multispecies Con-
612 nectivity Across a Transfrontier Conservation Landscape. *Journal of Applied Ecology*,
613 57:1700–1710.
- 614 Brooks, M. E., Kristensen, K., van Benthem, K. J., Magnusson, A., Berg, C. W., Nielsen,
615 A., Skaug, H. J., Maechler, M., and Bolker, B. M. (2017). glmmTMB Balances Speed and
616 Flexibility among Packages for Zero-Inflated Generalized Linear Mixed Modeling. *The R
617 Journal*, 9(2):378–400.
- 618 Brown, J. H. and Kodric-Brown, A. (1977). Turnover Rates in Insular Biogeography: Effect
619 of Immigration on Extinction. *Ecology*, 58(2):445–449.
- 620 Burnham, K. P. and Anderson, D. R. (2002). *Model Selection and Multimodel Inference: A
621 Practical Information-Theoretic Approach*. Springer Science & Business Media, Ney York,
622 NY, USA.
- 623 Börger, L. and Fryxell, J. (2012). Quantifying Individual Differences in Dispersal Using Net
624 Squared Displacement. In Clobert, J., Baguette, M., Benton, T. G., and Bullock, J. M.,
625 editors, *Dispersal Ecology and Evolution*. Oxford University Press, Oxford, UK.
- 626 Clark, J. D., Laufenberg, J. S., Davidson, M., and Murrow, J. L. (2015). Connectivity among
627 Subpopulations of Louisiana Black Bears as Estimated by a Step Selection Function. *The
628 Journal of Wildlife Management*, 79(8):1347–1360.

- 629 Cloibert, J., Baguette, M., Benton, T. G., and Bullock, J. M. (2012). *Dispersal Ecology and*
630 *Evolution*. Oxford University Press, Oxford, UK.
- 631 Cozzi, G., Behr, D., Webster, H., Claase, M., Bryce, C., Modise, B., McNutt, J., and
632 Ozgul, A. (2020). The Walk of Life: African Wild Dog Dispersal and its Implications for
633 Management and Conservation across Transfrontier Landscapes. In press.
- 634 Cozzi, G., Broekhuis, F., McNutt, J. W., Turnbull, L. A., Macdonald, D. W., and Schmid,
635 B. (2012). Fear of the Dark or Dinner by Moonlight? Reduced Temporal Partitioning
636 among Africa's Large Carnivores. *Ecology*, 93(12):2590–2599.
- 637 Cozzi, G., Maag, N., Börger, L., Clutton-Brock, T. H., and Ozgul, A. (2018). Socially
638 Informed Dispersal in a Territorial Cooperative Breeder. *Journal of Animal Ecology*,
639 87(3):838–849.
- 640 Creel, S., Merkle, J., Mweetwa, T., Becker, M. S., Mwape, H., Simpamba, T., and
641 Simukonda, C. (2020). Hidden Markov Models Reveal a clear Human Footprint on the
642 Movements of Highly Mobile African Wild Dogs. *Scientific reports*, 10(1):1–11.
- 643 Csardi, G. and Nepusz, T. (2006). The igraph Software Package for Complex Network
644 Research. *InterJournal*, Complex Systems:1695.
- 645 Cushman, S. A., Elliot, N. B., Bauer, D., Kesch, K., Bahaa-el din, L., Bothwell, H., Flyman,
646 M., Mtare, G., Macdonald, D. W., and Loveridge, A. J. (2018). Prioritizing Core Areas,
647 Corridors and Conflict Hotspots for Lion Conservation in Southern Africa. *PLOS ONE*,
648 13(7):e0196213.
- 649 Davies-Mostert, H. T., Kamler, J. F., Mills, M. G. L., Jackson, C. R., Rasmussen, G. S. A.,
650 Groom, R. J., and Macdonald, D. W. (2012). Long-Distance Transboundary Dispersal
651 of African Wild Dogs among Protected Areas in Southern Africa. *African Journal of
652 Ecology*, 50(4):500–506.
- 653 Diniz, M. F., Cushman, S. A., Machado, R. B., and De Marco Júnior, P. (2019). Landscape
654 Connectivity Modeling from the Perspective of Animal Dispersal. *Landscape Ecology*,
655 35:41–58.
- 656 Doerr, V. A. J., Barrett, T., and Doerr, E. D. (2011). Connectivity, Dispersal Behaviour
657 and Conservation under Climate Change: A Response to Hodgson et al.: Connectivity
658 and Dispersal Behaviour. *Journal of Applied Ecology*, 48(1):143–147.
- 659 Dwernychuk, L. W. and Boag, D. A. (1972). Ducks Nesting in Association with Gulls - An
660 Ecological Trap? *Canadian Journal of Zoology*, 50(5):559–563. Publisher: NRC Research
661 Press.
- 662 Eddelbuettel, D. (2013). *Seamless R and C++ Integration with Rcpp*. Springer, New York.
663 ISBN 978-1-4614-6867-7.
- 664 Eddelbuettel, D. and François, R. (2011). Rcpp: Seamless R and C++ Integration. *Journal
665 of Statistical Software*, 40(8):1–18.
- 666 Elliot, N. B., Cushman, S. A., Macdonald, D. W., and Loveridge, A. J. (2014). The Devil
667 is in the Dispersers: Predictions of Landscape Connectivity Change with Demography.
668 *Journal of Applied Ecology*, 51(5):1169–1178.
- 669 Fahrig, L. (2003). Effects of Habitat Fragmentation on Biodiversity. *Annual Review of
670 Ecology, Evolution, and Systematics*, 34(1):487–515.
- 671 Fieberg, J., Signer, J., Smith, B., and Avgar, T. (2021). A 'How to' Guide for Interpreting
672 Parameters in Habitat-Selection Analyses. *Journal of Animal Ecology*, 90(5):1027–1043.
- 673 Fortin, D., Beyer, H. L., Boyce, M. S., Smith, D. W., Duchesne, T., and Mao, J. S. (2005).
674 Wolves Influence Elk Movements: Behavior Shapes a Trophic Cascade in Yellowstone
675 National Park. *Ecology*, 86(5):1320–1330.

- 676 Fortin, D., Fortin, M.-E., Beyer, H. L., Duchesne, T., Courant, S., and Dancose, K. (2009).
677 Group-Size-Mediated Habitat Selection and Group Fusion–Fission Dynamics of Bison
678 under Predation Risk. *Ecology*, 90(9):2480–2490.
- 679 Frankham, R., Briscoe, D. A., and Ballou, J. D. (2002). *Introduction to Conservation
680 Genetics*. Cambridge University Press, Cambridge, UK.
- 681 Gastón, A., Blázquez-Cabrera, S., Garrote, G., Mateo-Sánchez, M. C., Beier, P., Simón,
682 M. A., and Saura, S. (2016). Response to Agriculture by a Woodland Species Depends on
683 Cover Type and Behavioural State: Insights from Resident and Dispersing Iberian Lynx.
684 *Journal of Applied Ecology*, 53(3):814–824.
- 685 Hanski, I. (1999). *Metapopulation Ecology*. Oxford University Press.
- 686 Hauenstein, S., Fattebert, J., Grüebler, M. U., Naef-Daenzer, B., Pe'er, G., and Hartig, F.
687 (2019). Calibrating an Individual-Based Movement Model to Predict Functional Connec-
688 tivity for Little Owls. *Ecological Applications*, 29(4):e01873.
- 689 Hijmans, R. J. (2021). *terra: Spatial Data Analysis*. R package version 1.2-10.
- 690 Hodel, F. H. and Fieberg, J. R. (2021a). Circular-linear copulae for animal movement data.
691 *bioRxiv*.
- 692 Hodel, F. H. and Fieberg, J. R. (2021b). Cyclop: An r package for circular-linear copulae
693 with angular symmetry. *bioRxiv*.
- 694 Hofmann, D. D., Behr, D. M., McNutt, J. W., Ozgul, A., and Cozzi, G. (2021). Bound
695 within Boundaries: How Well Do Protected Areas Match Movement Corridors of their
696 Most Mobile Protected Species? *Journal of Applied Ecology*. (in 2nd review).
- 697 Hunziker, P. (2021). *velox: Fast Raster Manipulation and Extraction*. R package version
698 0.2.1.
- 699 Kanagaraj, R., Wiegand, T., Kramer-Schadt, S., and Goyal, S. P. (2013). Using Individual-
700 Based Movement Models to Assess Inter-Patch Connectivity for Large Carnivores in Frag-
701 mented Landscapes. *Biological Conservation*, 167:298 – 309.
- 702 Keeley, A. T., Beier, P., Keeley, B. W., and Fagan, M. E. (2017). Habitat Suitability is a Poor
703 Proxy for Landscape Connectivity during Dispersal and Mating Movements. *Landscape
704 and Urban Planning*, 161:90–102.
- 705 Koen, E. L., Bowman, J., Sadowski, C., and Walpole, A. A. (2014). Landscape Connectivity
706 for Wildlife: Development and Validation of Multispecies Linkage Maps. *Methods in
707 Ecology and Evolution*, 5(7):626–633.
- 708 Koen, E. L., Garraway, C. J., Wilson, P. J., and Bowman, J. (2010). The Effect of Map
709 Boundary on Estimates of Landscape Resistance to Animal Movement. *PLOS ONE*,
710 5(7):e11785.
- 711 Kramer-Schadt, S., Revilla, E., Wiegand, T., and Grimm, V. (2007). Patterns for Parameters
712 in Simulation Models. *Ecological Modelling*, 204(3-4):553–556.
- 713 Latham, A. D. M., Latham, M. C., Boyce, M. S., and Boutin, S. (2011). Movement Re-
714 sponses by Wolves to Industrial Linear Features and Their Effect on Woodland Caribou
715 in Northeastern Alberta. *Ecological Applications*, 21(8):2854–2865.
- 716 Leigh, K. A., Zenger, K. R., Tammen, I., and Raadsma, H. W. (2012). Loss of Genetic
717 Diversity in an Outbreeding Species: Small Population Effects in the African Wild Dog
718 (*Lycaon pictus*). *Conservation Genetics*, 13(3):767–777.
- 719 MacArthur, R. H. and Wilson, E. O. (2001). *The Theory of Island Biogeography*, volume 1.
720 Princeton University Press, Princeton, New Jersey, USA.

- 721 Martensen, A. C., Saura, S., and Fortin, M. (2017). Spatio-Temporal Connectivity: Assessing
 722 the Amount of Reachable Habitat in Dynamic Landscapes. *Methods in Ecology and Evolution*, 8(10):1253–1264.
- 724 Masenga, E. H., Jackson, C. R., Mjingo, E. E., Jacobson, A., Riggio, J., Lyamuya, R. D.,
 725 Fyumagwa, R. D., Borner, M., and Røskift, E. (2016). Insights into Long-Distance
 726 Dispersal by African Wild Dogs in East Africa. *African Journal of Ecology*, 54(1):95–98.
- 727 McClure, M. L., Hansen, A. J., and Inman, R. M. (2016). Connecting Models to Movements:
 728 Testing Connectivity Model Predictions against Empirical Migration and Dispersal Data.
 729 *Landscape Ecology*, 31(7):1419–1432.
- 730 McNutt, J. (1996). Sex-Biased Dispersal in African Wild Dogs (*Lycaon pictus*). *Animal Behaviour*, 52(6):1067–1077.
- 732 McRae, B. H. (2006). Isolation by Resistance. *Evolution*, 60(8):1551–1561.
- 733 McRae, B. H., Dickson, B. G., Keitt, T. H., and Shah, V. B. (2008). Using Circuit Theory to
 734 Model Connectivity in Ecology, Evolution, and Conservation. *Ecology*, 89(10):2712–2724.
- 735 Morales, J. M., Haydon, D. T., Frair, J., Holsinger, K. E., and Fryxell, J. M. (2004).
 736 Extracting More out of Relocation Data: Building Movement Models as Mixtures of
 737 Random Walks. *Ecology*, 85(9):2436–2445.
- 738 Muff, S., Signer, J., and Fieberg, J. (2020). Accounting for Individual-Specific Variation in
 739 Habitat-Selection Studies: Efficient Estimation of Mixed-Effects Models Using Bayesian
 740 or Frequentist Computation. *Journal of Animal Ecology*, 89(1):80–92.
- 741 Nathan, R. (2008). An Emerging Movement Ecology Paradigm. *Proceedings of the National
 742 Academy of Sciences*, 105(49):19050–19051.
- 743 Osipova, L., Okello, M. M., Njumbi, S. J., Ngene, S., Western, D., Hayward, M. W., and
 744 Balkenhol, N. (2019). Using Step-Selection Functions to Model landscape Connectivity
 745 for African Elephants: Accounting for Variability across Individuals and Seasons. *Animal
 746 Conservation*, 22(1):35–48.
- 747 O'Neill, H. M. K., Durant, S. M., and Woodroffe, R. (2020). What Wild Dogs Want: Habitat
 748 Selection Differs across Life Stages and Orders of Selection in a Wide-Ranging Carnivore.
 749 *BMC Zoology*, 5(1).
- 750 Perrin, N. and Mazalov, V. (1999). Dispersal and Inbreeding Avoidance. *The American
 751 Naturalist*, 154(3):282–292.
- 752 Perrin, N. and Mazalov, V. (2000). Local Competition, Inbreeding, and the Evolution of
 753 Sex-Biased Dispersal. *The American Naturalist*, 155(1):116–127.
- 754 Pe'er, G. and Kramer-Schadt, S. (2008). Incorporating the Perceptual Range of Animals
 755 into Connectivity Models. *Ecological Modelling*, 213(1):73–85.
- 756 Pomilia, M. A., McNutt, J. W., and Jordan, N. R. (2015). Ecological Predictors of African
 757 Wild Dog Ranging Patterns in Northern Botswana. *Journal of Mammalogy*, 96(6):1214–
 758 1223.
- 759 Potts, J. R., Bastille-Rousseau, G., Murray, D. L., Schaefer, J. A., and Lewis, M. A. (2013).
 760 Predicting local and non-local effects of resources on animal space use using a mechanistic
 761 step selection model. *Methods in Ecology and Evolution*, 5(3):253–262.
- 762 Prokopenko, C. M., Boyce, M. S., and Avgar, T. (2017). Characterizing Wildlife Behavioural
 763 Responses to Roads Using Integrated Step Selection Analysis. *Journal of Applied Ecology*,
 764 54(2):470–479.
- 765 R Core Team (2020). *R: A Language and Environment for Statistical Computing*. R Foundation
 766 for Statistical Computing, Vienna, Austria.

- 767 Rudnick, D., Ryan, S., Beier, P., Cushman, S., Dieffenbach, F., Epps, C., Gerber, L., Hart-
768 ter, J., Jenness, J., Kintsch, J., Merenlender, A., Perkl, R., Perziosi, D., and Trombulack,
769 S. (2012). The Role of Landscape Connectivity in Planning and Implementing Conserva-
770 tion and Restoration Priorities. *Issues in Ecology*.
- 771 Sawyer, S. C., Epps, C. W., and Brashares, J. S. (2011). Placing Linkages among Fragmented
772 Habitats: Do Least-Cost Models Reflect How Animals Use Landscapes? *Journal of*
773 *Applied Ecology*, 48(3):668–678.
- 774 Signer, J., Fieberg, J., and Avgar, T. (2017). Estimating Utilization Distributions from
775 Fitted Step-Selection Functions. *Ecosphere*, 8(4):e01771.
- 776 Squires, J. R., DeCesare, N. J., Olson, L. E., Kolbe, J. A., Hebblewhite, M., and Parks, S. A.
777 (2013). Combining Resource Selection and Movement Behavior to Predict Corridors for
778 Canada Lynx at their Southern Range Periphery. *Biological Conservation*, 157:187–195.
- 779 Tischendorf, L. and Fahrig, L. (2000). On the Usage and Measurement of Landscape Con-
780 nectivity. *Oikos*, 90(1):7–19.
- 781 Turchin, P. (1998). *Quantitative Analysis of Movement: Measuring and Modeling Population*
782 *Redistribution in Plants and Animals*. Sinauer Associates, Sunderland, MA, USA.
- 783 Van der Meer, E., Fritz, H., Blinston, P., and Rasmussen, G. S. (2014). Ecological Trap in
784 the Buffer Zone of a Protected Area: Effects of Indirect Anthropogenic Mortality on the
785 African Wild Dog (*Lycaon pictus*). *Oryx*, 48(2):285–293.
- 786 Vasudev, D., Fletcher, R. J., Goswami, V. R., and Krishnadas, M. (2015). From Disper-
787 sal Constraints to Landscape Connectivity: Lessons from Species Distribution Modeling.
788 *Ecography*, 38(10):967–978.
- 789 Wiegand, T., Jeltsch, F., Hanski, I., and Grimm, V. (2003). Using Pattern-Oriented Mod-
790 eling for Revealing Hidden Information: A Key for Reconciling Ecological Theory and
791 Application. *Oikos*, 100(2):209–222.
- 792 Wolski, P., Murray-Hudson, M., Thito, K., and Cassidy, L. (2017). Keeping it Simple:
793 Monitoring Flood Extent in Large Data-Poor Wetlands Wsing MODIS SWIR Data. *In-*
794 *ternational Journal of Applied Earth Observation and Geoinformation*, 57:224–234.
- 795 Woodroffe, R. and Ginsberg, J. R. (1999). Conserving the African Wild Dog *Lycaon pictus*.
796 Diagnosing and Treating Causes of Decline. *Oryx*, 33(2):132–142.
- 797 Woodroffe, R., Rabaiotti, D., Ngatia, D. K., Smallwood, T. R. C., Strelbel, S., and O'Neill,
798 H. M. K. (2019). Dispersal Behaviour of African Wild Dogs in Kenya. *African Journal*
799 *of Ecology*.
- 800 Woodroffe, R. and Sillero-Zubiri, C. (2012). *Lycaon pictus*. *The IUCN Red List of Threatened*
801 *Species*, 2012:e. T12436A1671116.
- 802 Zeller, K. A., McGarigal, K., and Whiteley, A. R. (2012). Estimating Landscape Resistance
803 to Movement: A Review. *Landscape Ecology*, 27(6):777–797.
- 804 Zeller, K. A., Wattles, D. W., Bauder, J. M., and DeStefano, S. (2020). Forecasting Seasonal
805 Habitat Connectivity in a Developing Landscape. *Land*, 9(7):233.

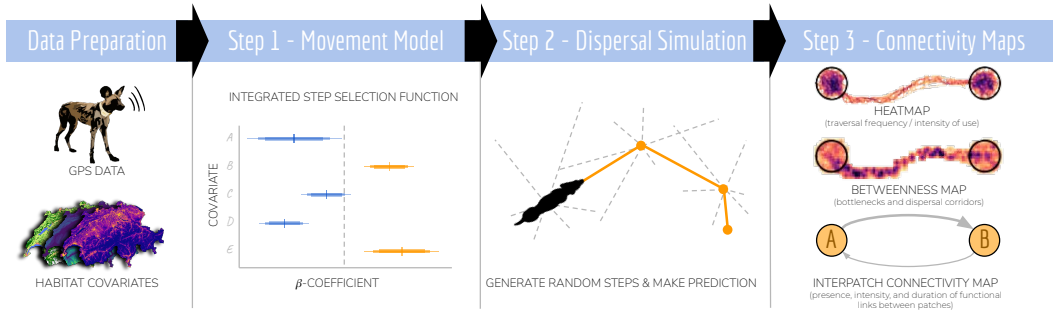


Figure 1: Flowchart of the simulation-based connectivity analysis as proposed in this article. First, GPS data and habitat covariates have to be collected. The combined data is then analyzed in an integrated step selection model, which enables the parametrization of the focal species' habitat and movement kernels and results in a mechanistic movement model. The parametrized model is then treated as an individual-based movement model and used to simulate dispersal trajectories. Ultimately, simulated trajectories serve to produce a set of maps that are pertinent to landscape connectivity. This includes a heatmap, indicating the traversal frequency across each spatial unit of the study area, a betweenness map, highlighting movement corridors and bottlenecks, and, finally, an inter-patch connectivity map, where the frequency of connections and their average duration can be depicted.

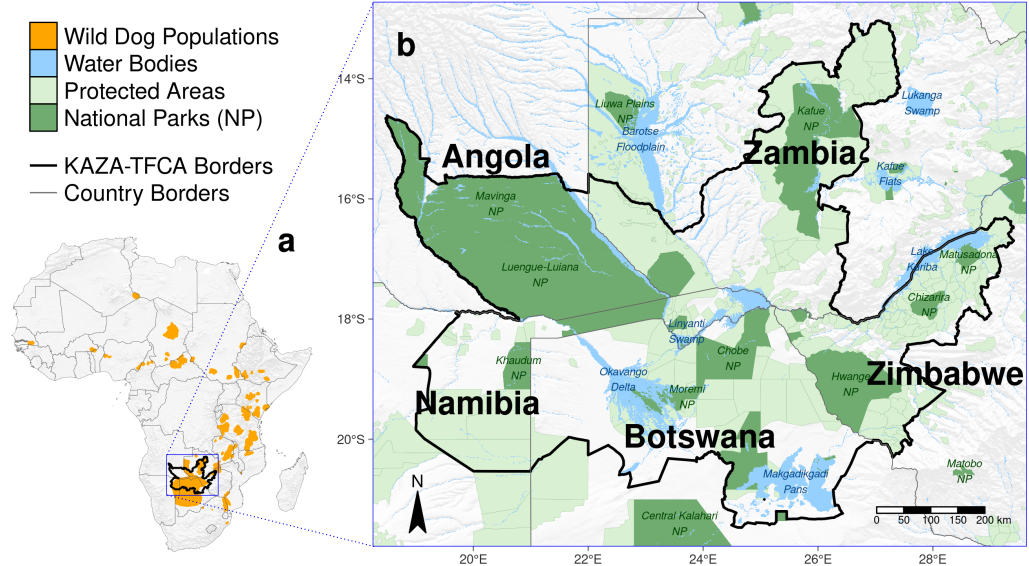


Figure 2: Illustration of the study area located in southern Africa. (a) The study area was confined by a bounding box spanning the entire KAZA-TFCA and comprised parts of Angola, Namibia, Botswana, Zimbabwe, and Zambia. (b) The KAZA-TFCA represents the world's largest terrestrial conservation area and covers a total of 520'000 km². Its main purpose is to re-establish connectivity between already-existing national parks (dark green) and other protected areas (light green).

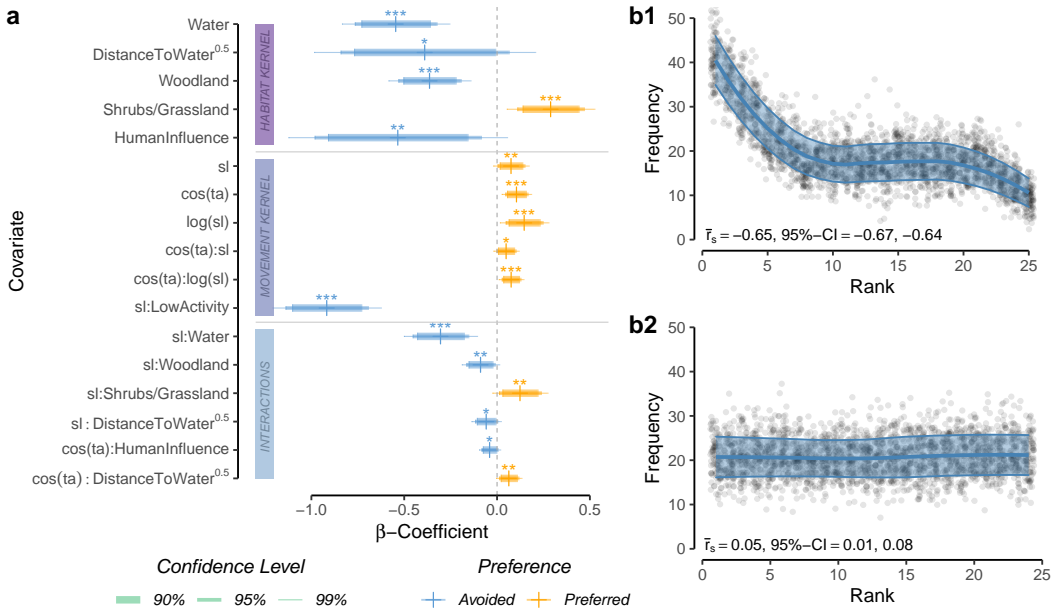


Figure 3: (a) Most parsimonious movement model for dispersing wild dogs. The model comprises a habitat kernel, a movement kernel, as well as their interactions. The horizontal line segments delineate the 90%, 95%, and 99% confidence-intervals for the respective β -coefficients. Significance codes: * $p < 0.10$, ** $p < 0.05$, *** $p < 0.01$. (b) Results from the k-fold cross validation procedure. The upper plot shows rank frequencies of realized steps according to model predictions with known preferences, whereas the lower plot shows rank frequencies of realized steps when assuming random preferences. The blue ribbon shows the prediction interval around a loess smoothing regression that we fitted to ease the interpretation of the plots. The significant correlation between rank and associated frequency in (b1) highlights that the most parsimonious model successfully outperforms a random guess (b2) and assigns comparably high selection scores to realized steps.

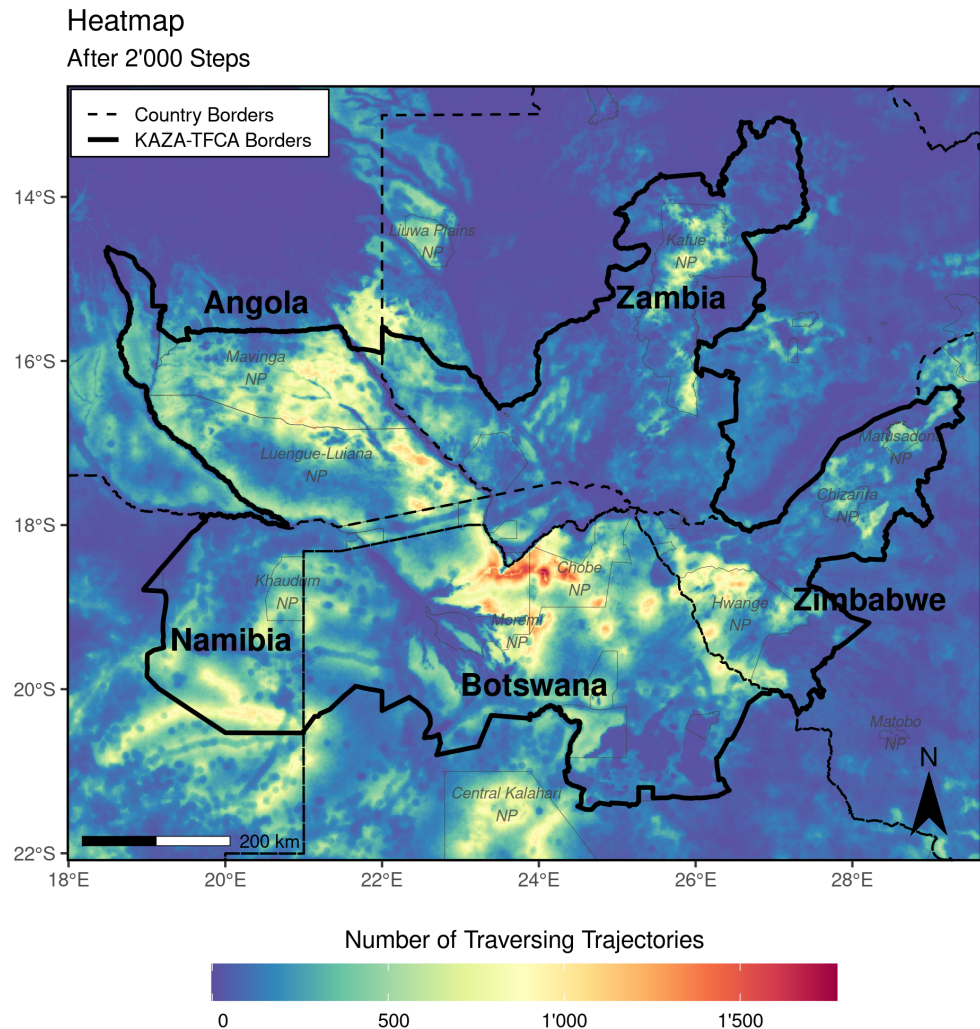


Figure 4: Heatmap showing traversal frequencies of 80'000 simulated dispersers moving 2'000 steps across the KAZA-TFCA. Simulations were based on an integrated step selection model that we fitted to the movement data of dispersing African wild dogs. To generate the heatmap, we rasterized and tallied all simulated trajectories. Consequently, the map highlights areas that are frequently traversed by virtual dispersers. For spatial reference we plotted a few selected national parks (dark gray). Additional heatmaps showing the traversal frequency when individuals move fewer than 2'000 steps are provided in Figure S4.

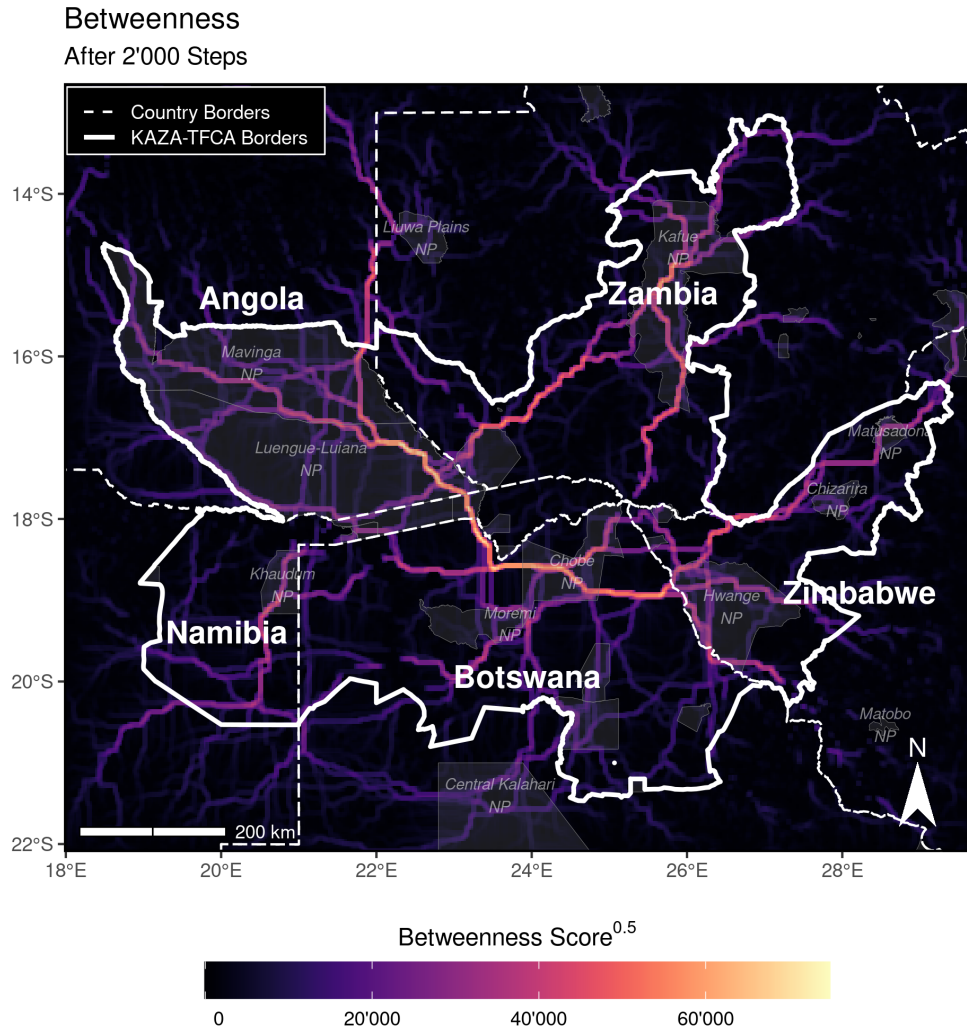


Figure 5: Map of betweenness scores, highlighting distinct dispersal corridors and potential bottlenecks across the extent of the KAZA-TFCA. A high betweenness score indicates that the respective area is exceptionally important for connecting different regions in the study area. In this sense the metric can be used to pinpoint discrete movement corridors (Bastille-Rousseau et al., 2018). Note that we square-rooted betweenness scores to improve visibility of corridors with low scores. Additional betweenness maps showing betweenness scores when individuals move fewer than 2'000 steps are provided in Figure S4.

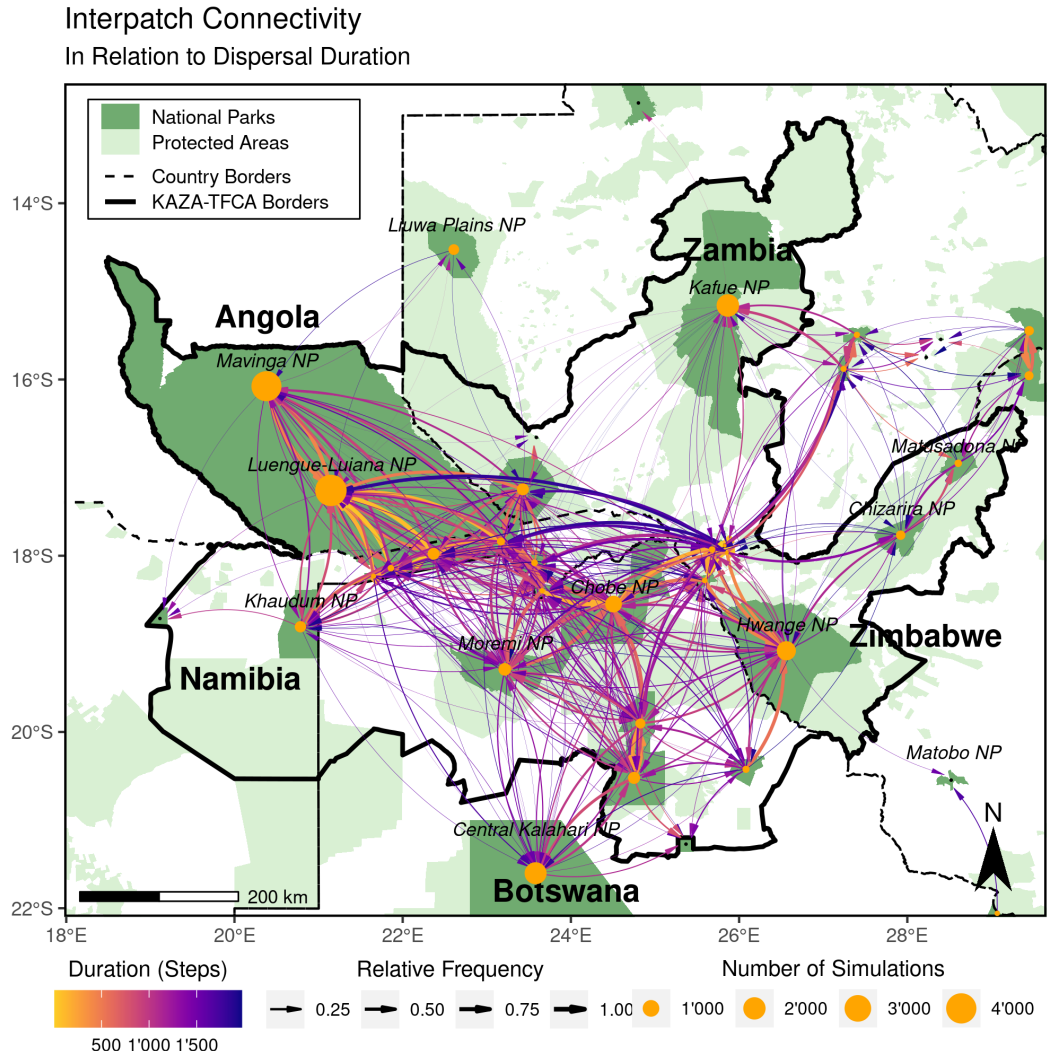


Figure 6: Map of inter-patch connectivity, highlighting connections between national parks (dark green). Yellow bubbles represent the center of the different national parks and are sized in relation to the number of simulated dispersers originating from each park. Black dots represent national parks that were smaller than 700 km^2 and therefore did not serve as source areas. Arrows between national parks illustrate between which national parks the simulated dispersers successfully moved and the color of each arrow shows the average number of steps (4-hourly movements) that were necessary to realize those connections. Additionally, the line thickness indicates the relative number of dispersers originating from a national park that realized those connections. Note that a similar network view could be adopted to investigate connectivity between other protected areas need not to be restricted to national parks.